

Excitation of long-period Rayleigh waves by large storms over the North Atlantic Ocean

Dieter Kurrle^{1*} and Rudolf Widmer-Schmidrig²

¹*Institute of Geophysics, University of Stuttgart, Azenbergstr. 16, D-70174 Stuttgart, Germany. E-mail: Dieter.Kurrle@lgrb.uni-freiburg.de*

²*Black Forest Observatory (BFO), Heubach 206, D-77709 Wolfach, Germany*

Accepted 2010 July 5. Received 2010 July 3; in original form 2009 December 18

SUMMARY

Marine microseisms are known to be the major source of seismic noise. Generally, ground motions in the frequency range between 0.05 and 1 Hz induced by ocean waves are referred to as microseisms. In this article we show that in addition to such microseisms, strong storms over the North Atlantic Ocean can also cause an increase of seismic noise at lower frequencies. As an example, a storm in 1999 October is analysed in detail. When the ocean waves caused by this storm hit the coastline, seismic Rayleigh waves with frequencies below 0.02 Hz were excited and could be observed globally. Using broad-band seismic networks in Germany and California as arrays, these Rayleigh waves can be traced back to the centre of the storm. Between 1999 and 2007, we identified more than 40 events with similar characteristics. Since it is expected that such storms also occur in other regions, it is likely that these storms together contribute significantly to the continuous excitation of the Earth's free oscillations, also known as the hum of the Earth.

Key words: Surface waves and free oscillations.

1 INTRODUCTION

Large ocean storms have been known to cause seismic noise more than 100 yr ago (Wiechert 1904). Nowadays seismic noise from oceanic disturbances is referred to as marine microseisms (e.g. Longuet-Higgins 1950; Hasselmann 1963). Usually one discriminates between two constituents of microseismic noise differing in frequency. The smaller primary microseisms are observed between 0.05 and 0.1 Hz, the larger peak in the noise spectra (e.g. Peterson 1993; Berger *et al.* 2004) which is called secondary microseisms occurs at twice the frequency of primary microseisms, between 0.1 and 0.2 Hz.

Since the frequency of primary microseisms agrees well with observed frequencies of oceanic swell, this kind of seismic noise is directly attributed to swell waves impinging on the coastlines. The frequency doubling of secondary microseisms was shown by Longuet-Higgins (1950) to be the result of non-linear interactions of ocean waves, either in coastal areas, where waves are partially reflected, or in the centre of cyclonic depressions.

While microseisms often show different spectral properties, depending on time and location of observation, all studies agree on a maximum period of about 25 s, corresponding to the maximum period of ocean swell. At longer periods, seismic noise decreases steeply and reaches a minimum around 0.015 Hz. For vertical seismic noise at quiet sites, another minimum near 3 mHz occurs due

to the cancellation of different effects caused by local atmospheric pressure fluctuations (Zürn & Wielandt 2007). At periods longer than 500 s, seismic noise increases again, primarily due to Newtonian attraction caused by moving air masses in the vicinity of a seismic station.

In 1998, Suda *et al.* showed that between 2 and 7 mHz it is possible to observe an excitation of spheroidal free oscillations of the Earth even in times devoid of large earthquakes (Suda *et al.* 1998). Since then, these background oscillations, also known as the 'hum of the Earth', have been studied intensively, however, their origin is still not known in detail. While first studies named atmospheric pressure fluctuations as the source of the hum (Kobayashi & Nishida 1998; Tanimoto & Um 1999; Fukao *et al.* 2002), more recent work indicates that oceanic infragravity waves (e.g. Webb *et al.* 1991) play a major role in the excitation process (Rhie & Romanowicz 2004, 2006; Tanimoto 2005; Webb 2007, 2008; Bromirski & Gerstoft 2009).

The Earth's hum observed on vertical component data from broad-band seismometers, spring and superconducting gravimeters almost exclusively consists of fundamental spheroidal modes. Beyond that, only a weak excitation of the first overtone branch could be shown (Fukao *et al.* 2002; Nishida *et al.* 2002). Recently, a permanent excitation of toroidal modes or, equivalently, Love waves was found (Kurrle & Widmer-Schmidrig 2008; Nishida *et al.* 2008). However, due to the much higher noise levels of horizontal component seismic data, we only consider spheroidal modes observed in vertical seismic data in this study.

As fundamental spheroidal modes can also be viewed as standing Rayleigh waves, several studies used a time-domain surface wave

*Now at: Landesamt für Geologie, Rohstoffe und Bergbau, Albertstr. 5, D-79104 Freiburg, Germany.

approach to identify the nature (Ekström 2001; Nishida *et al.* 2002) and to locate the sources (Rhie & Romanowicz 2004; Nishida & Fukao 2007) of the Earth's hum. A major observational feature indicating that the background oscillations are caused by atmospheric and/or oceanic disturbances is the presence of seasonal variations of both amplitudes (Tanimoto & Um 1999) and propagation directions of the background Rayleigh waves (Rhie & Romanowicz 2004; Kurrle & Widmer-Schmidrig 2006). Comparisons of the observed propagation directions with global distributions of ocean wave heights suggest a connection between ocean waves and the hum. Rhie & Romanowicz (2006) showed a close relationship between ocean waves arriving at the west coast of North America and long-period ($T > 100$ s) seismic Rayleigh waves observed across the entire continent. Recently, Bromirski & Gerstoft (2009) demonstrated that the hum observed with the USArray is mainly caused by infragravity waves near the western coast of North America and, to a smaller extent, the European coast.

In this paper, we confirm the western European coast as a source area of long-period seismic noise and show that for particularly large storms in the North Atlantic Ocean, the seismic noise caused by these storms has, beside 'conventional microseisms', an additional component at frequencies below 0.02 Hz. Using data from broad-band seismic stations in Germany and Luxemburg as well as in California, we identify this small portion of seismic noise as Rayleigh waves excited by ocean waves hitting the western European coast.

Starting in the early 1990s, a uniform network of broad-band seismic stations was established in Germany: The German Regional Seismic Network (GRSN). Meanwhile it consists of 19 stations, all except one of them are equipped with a Streckeisen STS-2 seismometer and a 24bit digitizer. In a previous study to investigate the long-term behaviour of the hum, we performed a frequency domain beamforming adjusted to the dispersion characteristics of

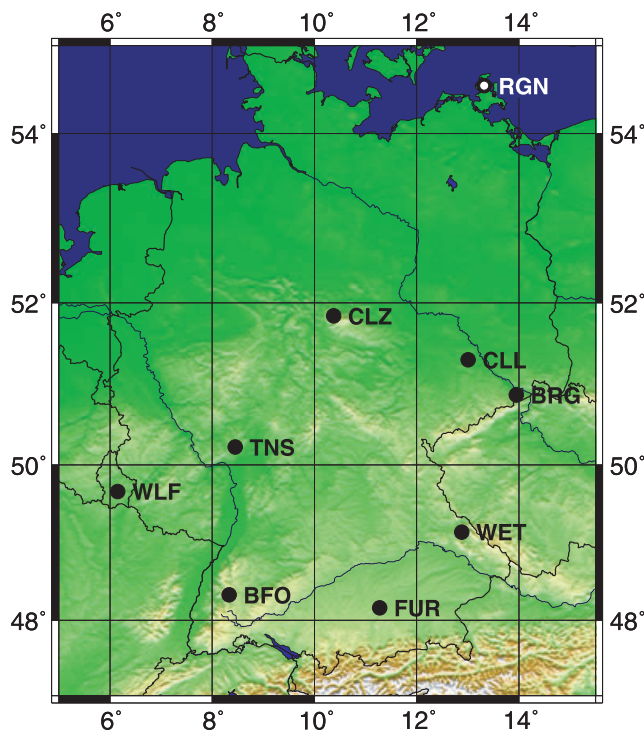


Figure 1. Station map of eight GRSN and one GEOFON stations used as seismic array.

Rayleigh waves on the vertical component data from eight GRSN stations and one GEOFON station in Luxemburg (see Fig. 1 and Kurrle & Widmer-Schmidrig 2006). In that paper, we were able to show that the propagation directions of background Rayleigh waves at periods between 125 and 200 s show seasonal variations with a high annual recurrence. However, due to the averaging over 10 d time windows, no information about the short-term characteristics of the background waves could be obtained. This is the scope of the present study.

2 A MICROSEISMIC STORM IN 1999 OCTOBER

From 1999 October 21–23, an increase of seismic noise was observed at all stations of the GRSN. Fig. 2 shows time-series from the nine stations in Fig. 1, bandpass filtered in the microseismic frequency band between 0.05 and 0.2 Hz. At all stations, the amplitudes increase simultaneously, thus local effects or instrumental disturbances can be excluded. The spectral composition of seismic noise during that period is shown in the left part of Fig. 3 for the GRSN station CLL. To highlight short-term variations, this spectrogram was 'pre-whitened' by subtracting the first quartile of acceleration power spectral density over the whole 10-d period (upper panel). In the right part of Fig. 3, a schematic view of the spectrogram is shown to indicate the most important features. The

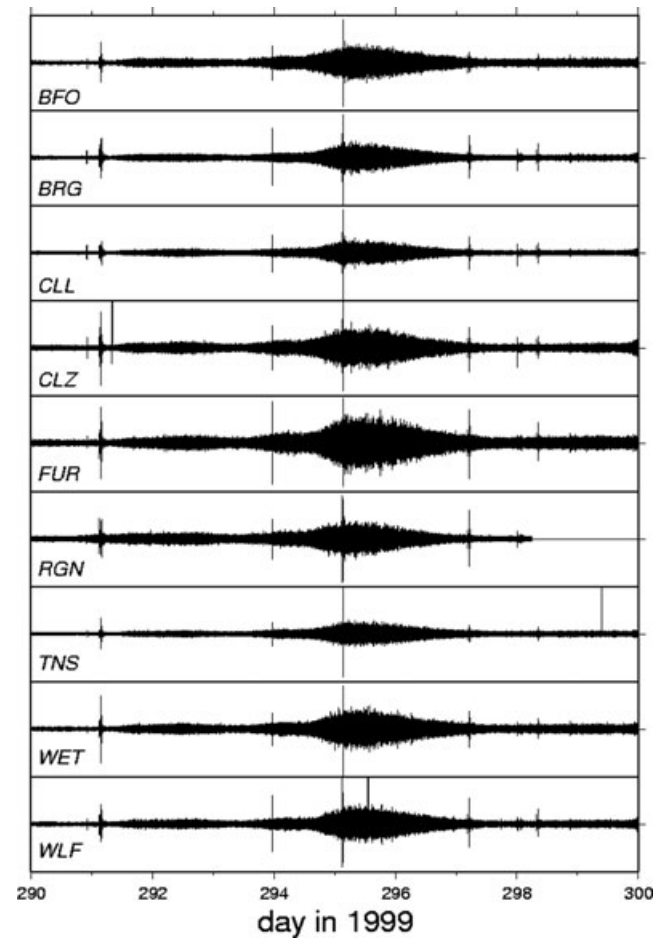


Figure 2. Vertical component seismograms for the time period 1999 October 17–October 26 (days 290–299). A strong microseismic event occurred on days 294–296. Data of station RGN are incomplete.

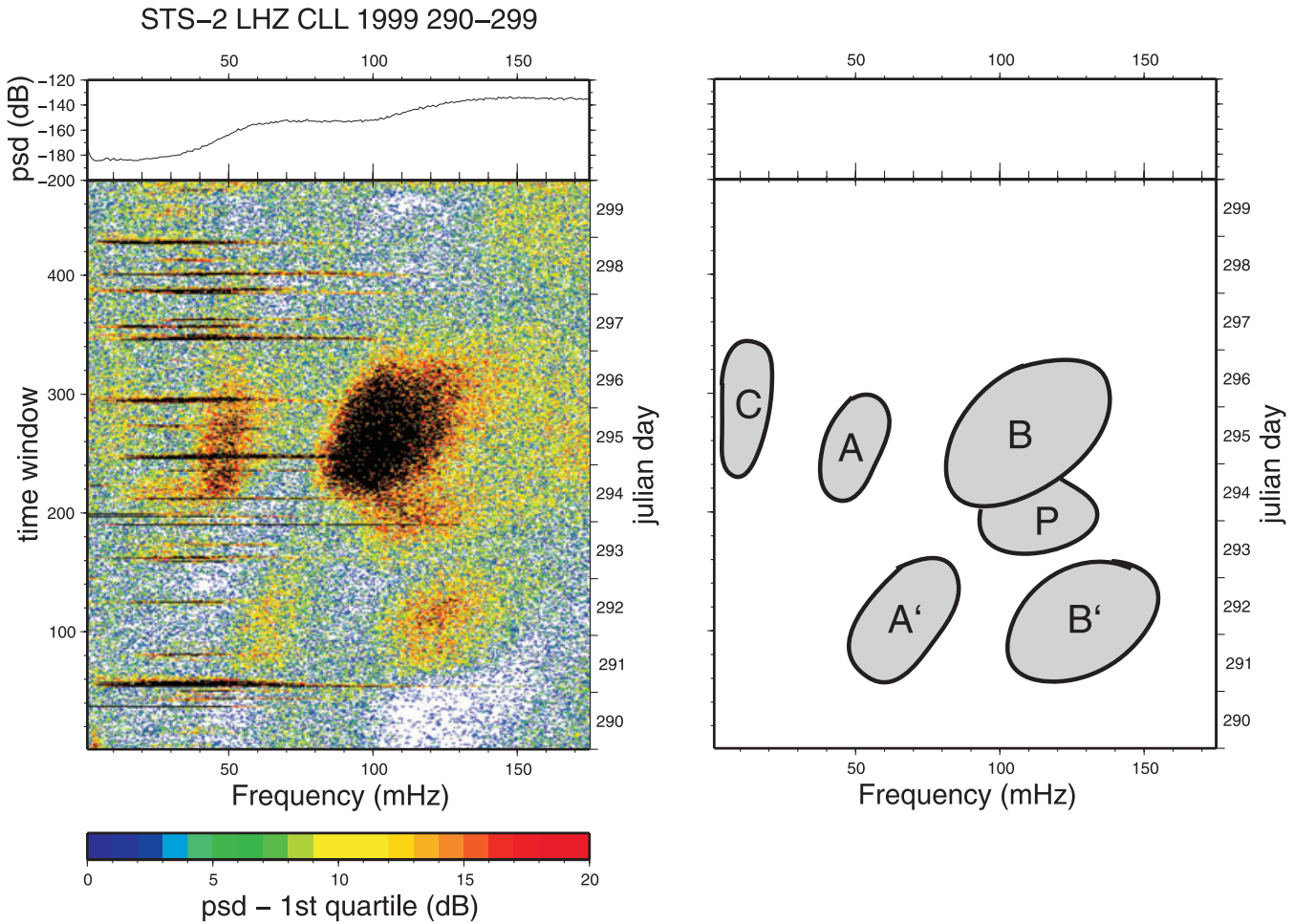


Figure 3. Left-hand panel: vertical component spectrogram for the GRSN station CLL. The time period is the same as in Fig. 2. Power spectral density (psd) is given in dB relative to $1 \text{ m}^2 \text{ s}^{-3}$. To reduce the amplitude range to plot and to enhance short-term fluctuations, the first quartile of acceleration power spectral density over the whole 10-d-period (upper panel) was subtracted. Right-hand panel: schematic view of important features; see text for details.

spectrogram reveals the main parts of this noise event as primary and secondary microseisms around 0.05 and 0.1 Hz, respectively (labels A and B). The onsets of both primary and secondary microseisms occur simultaneously on day 294 (October 21), around 12:00 UT, the duration of this event is about 2 d. A slight dispersion, that is, an increase of frequency with time, can be observed for this strong event as well as for a smaller one on days 291 and 292 (labels A' and B'). This smaller event shows similar characteristics, but at significantly higher frequencies (0.06 and 0.12 Hz). Horizontal stripes seen at frequencies below 0.1 Hz are due to teleseismic earthquakes, the largest one being a $M_W = 6.3$ event on day 291, 02:43 UT near the South Sandwich Islands.

Considering now the low-frequency band with $f < 0.02$ Hz, a maximum of seismic noise (label C) is observed on days 295 and 296 (October 22 and 23), having a duration of about 2 d and thus the same as the strong microseisms seen at higher frequencies. However, the long-period noise is delayed by about 12 hr with respect to microseisms. As will be discussed later, we have identified more than 40 events with similar characteristics over a period of 8.5 yr. The concurrent microseisms around 0.05 and 0.1 Hz, the delayed increase of noise at $f < 0.02$ Hz as well as the 'precursor' of secondary microseisms at slightly higher frequencies (label P) are typical features of these events and thus can give insights into the processes leading to the seismic excitation.

In (Kurrle & Widmer-Schmidrig 2006), we used the stations shown in Fig. 1 as an array to estimate the propagation direction of background Rayleigh waves. To do so, a frequency domain beamforming was conducted. We assumed plane wave propagation and the dispersion relation of Rayleigh waves given by PREM (Dziewonski & Anderson 1981). We computed the Fourier transform of the seismograms, applied phase shifts according to the propagation direction and calculated the power of the summed trace. A grid search over propagation directions for sliding time windows then yielded the distribution of beam power over backazimuths and time.

Such a beam power distribution is shown in Fig. 4 for the 10 d interval in 1999 October. The calculation was carried out for time windows of 3 hr length and 2 hr overlap. Beam power was calculated in the frequency domain and integrated from 5 to 8 mHz, since the wavelengths corresponding to this frequency range (about 500–900 km) are best suited for an array analysis with these stations. The maximum beam power over the whole time span was normalized to 1.

Rayleigh waves from earthquakes can be seen as horizontal lines of high beam power, most of them having backazimuths smaller than 100° . These earthquakes are short, transient phenomena with a duration of at most 3 hr. In addition, however, a long-standing period of increased beam power can be identified for backazimuths

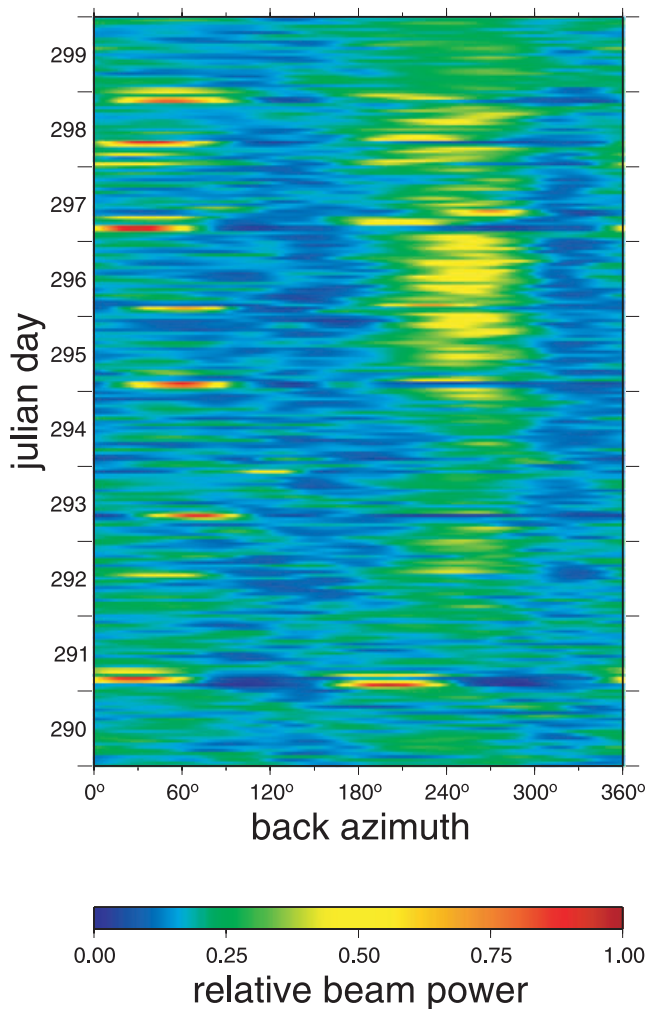


Figure 4. Result of beamforming in the frequency range 5–8 mHz using the stations in Fig. 1. Beam power is normalized to a maximum value of 1.

near 250° on days 295 and 296, while the onset is steeper than the decay. The comparison with Fig. 3 shows that this broad maximum of beam power corresponds to the elevated long-period noise in the spectrogram.

The propagation direction of the Rayleigh waves seen in Fig. 4 suggests a source to the west of Germany. Since it is not possible to determine the distance to the source of these surface waves with only one array, we need at least one additional array to narrow down the source area. In (Rhie & Romanowicz 2004), data from two broad-band seismic networks were used to locate the sources of background Rayleigh waves: The Japanese F-net and the Berkeley Digital Seismic Network (BDSN). While the BDSN consisted of about 30 stations at that time, they used only the seven least noisy of them. For the particular period in 1999 October we found—except for one, we used SAO instead of MOD—the same stations to be suitable to study the seismic noise at very long periods. A station map is shown in Fig. 5. The station WDC was equipped with an STS-2 seismometer, the others with STS-1 seismometers.

Fig. 6 shows a spectrogram, similar to that in Fig. 3, for the BDSN station ORV. The most outstanding difference between the two spectrograms is the almost complete lack of secondary microseisms at ORV (label B in Fig. 3). In contrast, the primary microseismic peak in the spectrogram for the station ORV is very similar

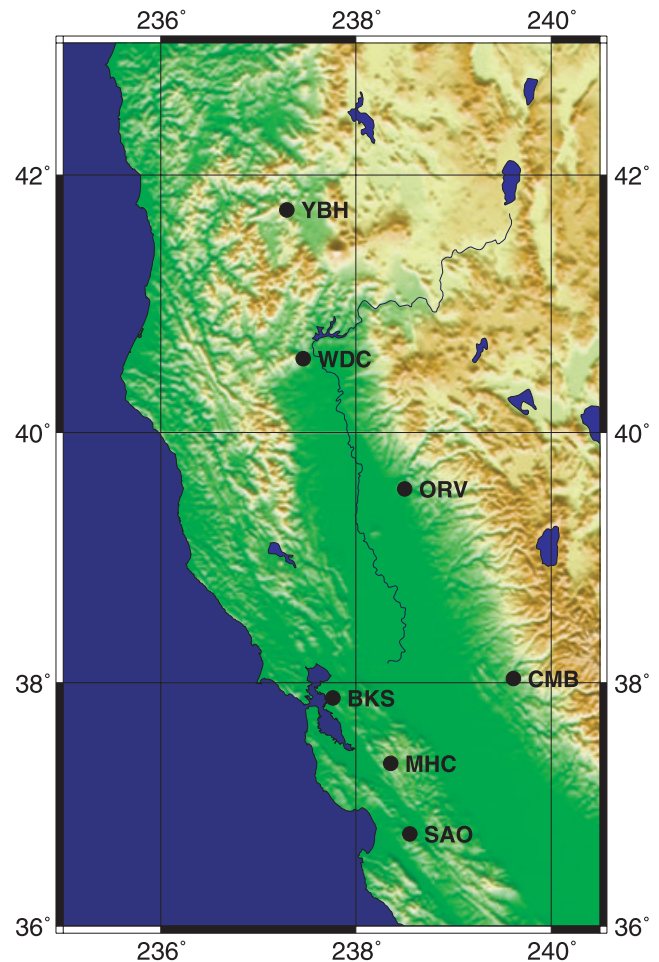


Figure 5. Map of BDSN stations used to determine the propagation direction of background Rayleigh waves.

to that observed at CLL. Finally, the increase of long-period noise at frequencies below 0.02 Hz is also observable in both spectrograms.

As for the GRSN stations, we tried to estimate the propagation direction of Rayleigh waves by performing a frequency-domain beamforming. Unfortunately, the subnetwork of the BDSN is less suited as array for long-period surface waves as the German network, due to its different extensions in north–south and east–west direction. There are no large sidelobes in the array response function, but the width of the central maximum in east–west direction is about three times the width in north–south direction. Thus, an ambiguity for waves deviating by the same angle from an east–west propagation is expected, similar to a linear, one-dimensional array.

The beamforming result is shown in Fig. 7. The picture is much less clear than Fig. 4, an axial symmetry with respect to a backazimuth of 170° is evident. Beside short transient maxima of beam power caused by earthquakes, the most prominent feature is a maximum on day 295 (October 22), lasting at least 24 hr and having a backazimuth of about 50°. Due to its slightly higher amplitude, we regard this maximum as the ‘true’ one instead of that near 290° which is probably an artefact of the unfavourable array response.

Having now obtained two independent estimates of the propagation directions of the long-period Rayleigh waves related to this particular event, we can combine both bearings and perform a triangulation to determine the source region. To do so, we carried out a grid search over all possible source locations for both arrays. Since earthquakes cause much higher beam power than the microseismic

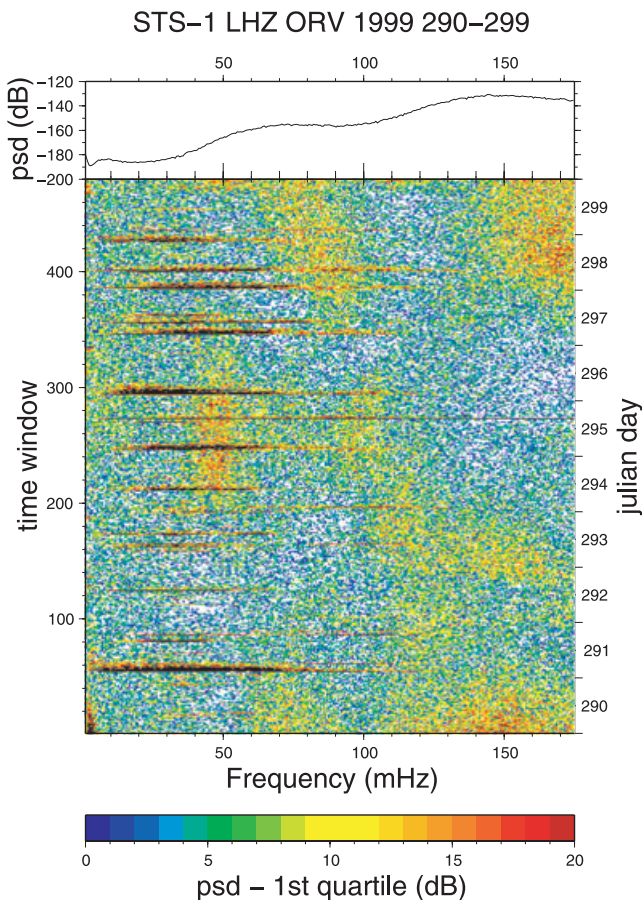


Figure 6. Vertical component spectrogram for the BDSN station ORV, equivalent to Fig. 3.

storm, we excluded time windows contaminated by earthquakes and averaged over ‘quiet’ time windows for each day. Afterwards, the beam power estimates obtained with the two arrays were multiplied for each gridpoint and normalized to a total maximum of 1. By multiplying two independent results, we try to focus on common source areas and to suppress those sources which can only be detected with one of the arrays.

The daily estimates of source locations are shown on the left side of Fig. 8 from 1999 October 20 (day 293) to October 25 (day 298). On the right-hand side, global distributions of significant wave height are shown, reproduced from wave action model (WAM; WAMDI group 1988) nowcasts for 12:00 UT.

While on days 293 and 294, no significant seismic sources can be detected, a large storm causing extreme wave heights higher than 15 m is evident in the WAM maps. Only on day 295, when the centre of the storm, still producing wave heights up to 10 m, reaches regions of shallower water depths near the European coast, long-period seismic waves are observed. The correspondence of the areas of maximum wave height and maximum beam power is striking. However, with respect to the days before, the beam power on day 295 is increased for the whole Earth, especially for a region spanning South America and parts of the Southeast Pacific Ocean. As seen from the German stations, these regions lie in the same direction as the main spot in the North Atlantic Ocean. Thus it is not possible to further constrain the source locations only with the data from this array. As was shown in Fig. 7, the beam power distribution obtained from the BDSN data is more complex than that from the GRSN. Only for a few azimuths and time windows, the

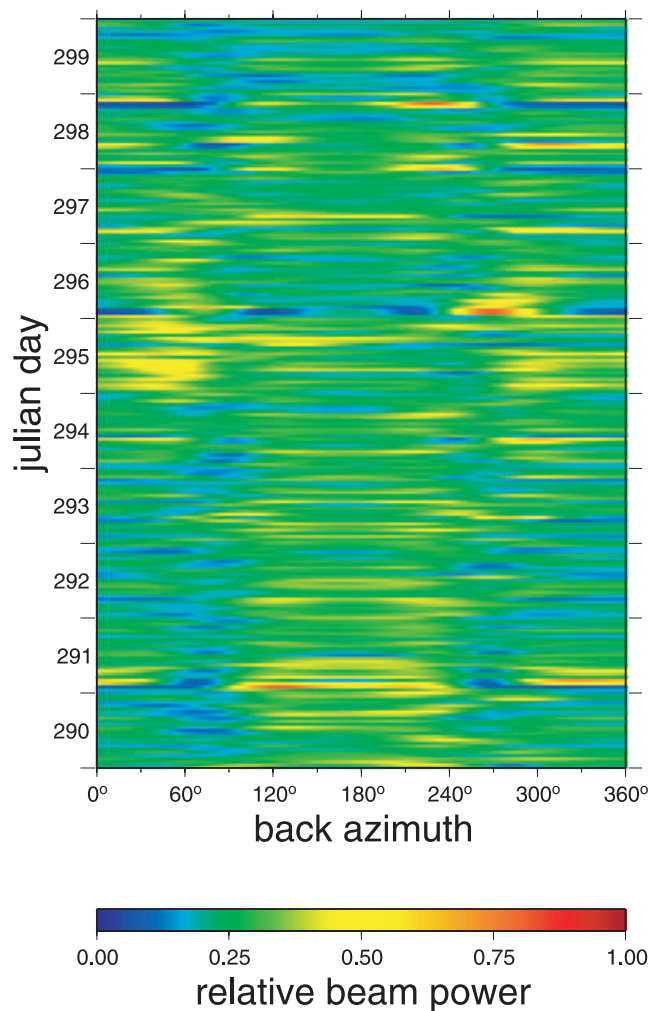


Figure 7. Same as in Fig. 4, but for the BDSN stations shown in Fig. 5.

beam power falls below 0.3. Most likely, the multiplication of high beam power from the GRSN with this more uniform ‘background’ beam power from the BDSN stations causes the apparent seismic excitation source over South America.

On days 296 and 297, the estimated beam power and significant wave heights decrease concurrently, but still show a maximum in the Atlantic Ocean. This development clearly coincides with the onset and decay of long-period noise seen in Figs 3 and 4, showing that the enhanced power spectral density at long periods in the spectrograms is caused by surface waves excited by the storm in the North Atlantic Ocean hitting the European coast.

For reference, we used the same method and the same stations to locate a $M_W = 4.9$ earthquake near the Azores Islands on 1996 March 9. The result given in Fig. 9 is very similar to that in Fig. 8 for day 295. The maximum of beam power is close to the source (marked by a star), but there is the same elevation of beam power for South America and parts of the southeast Pacific Ocean. This shows that in fact the seismic waves observed during the storm in 1999 October were excited in the North Atlantic Ocean and that the apparent source over South America is an artefact of the location method and the station distribution.

To further constrain time and location of the seismic excitation during the storm, it would be helpful to compare the time history of the ocean waves with that of the seismic waves. Knowledge about ocean waves is best provided by time-series from meteorological

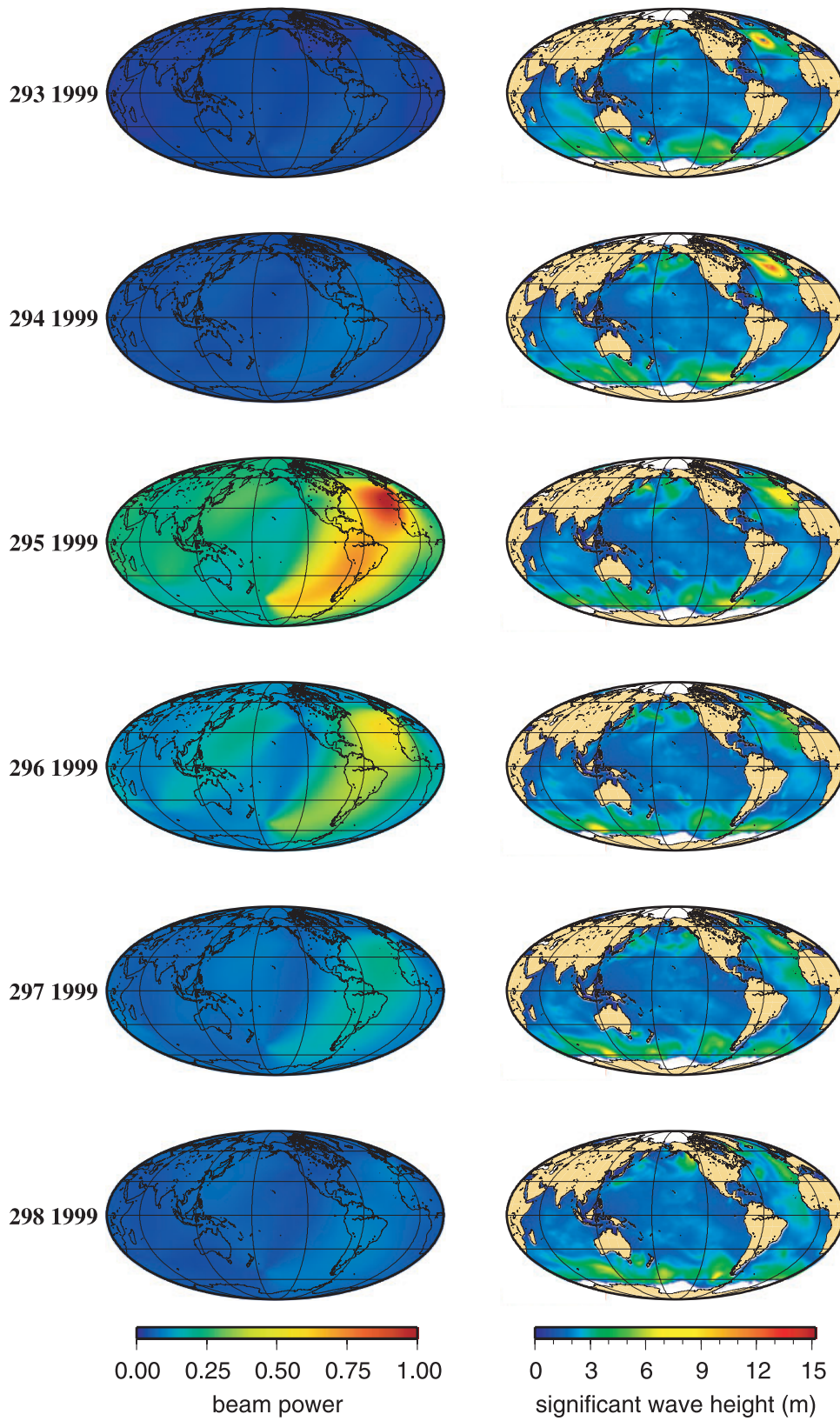


Figure 8. Comparison between daily averages of seismic beam power estimates (left-hand panel) and global ocean wave action models (WAM) of significant wave height (right-hand panel).

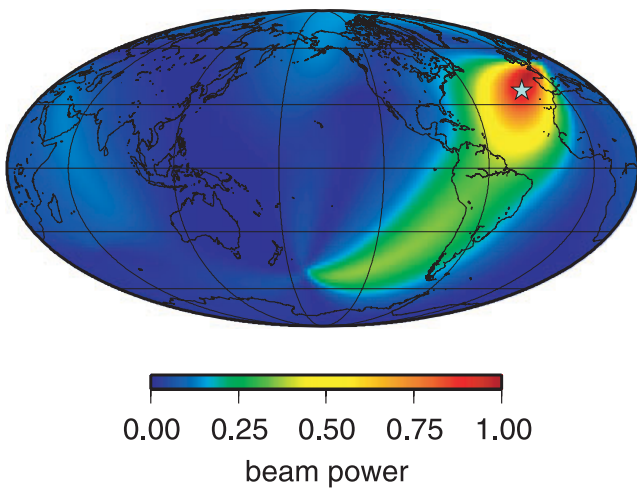


Figure 9. Result of beamforming for a $M_W = 4.9$ earthquake near the Azores (epicentre marked by a star) on March 9, 1996.

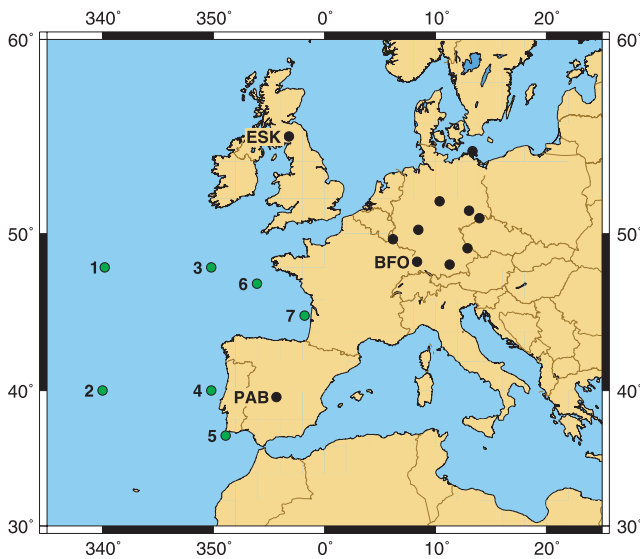


Figure 10. Map showing seismic stations (black dots) and locations where significant wave heights were estimated (green dots). Stations without labels are those shown in Fig. 1.

buoys. Since we did not have access to data from the few, sparsely distributed buoys in the area of interest, we went back to the global wave height models as shown in Fig. 8 and extracted time-series of significant wave heights at selected locations. Of course, wave heights obtained from these models can differ significantly from those a real buoy would measure at the same location, and the time resolution of 12 hr is rather poor. On the other hand, the buoy data are assimilated into the WAMs, and referring to the global models allows us to freely select the points of observation.

We selected seven locations in the North Atlantic Ocean where we extracted significant wave height time-series from the global models. These locations are displayed in Fig. 10. Also shown are the locations of three seismic observatories and the stations used as array. In Fig. 11, we compare the significant wave heights with the seismic noise levels averaged for periods between 100 and 200 s at these three stations. At first, the significant wave height rises at the most western points 1 and 2. Then the other locations follow in ascending order. The seismic noise at PAB increases at the same time as the significant wave heights determined at points 4 and

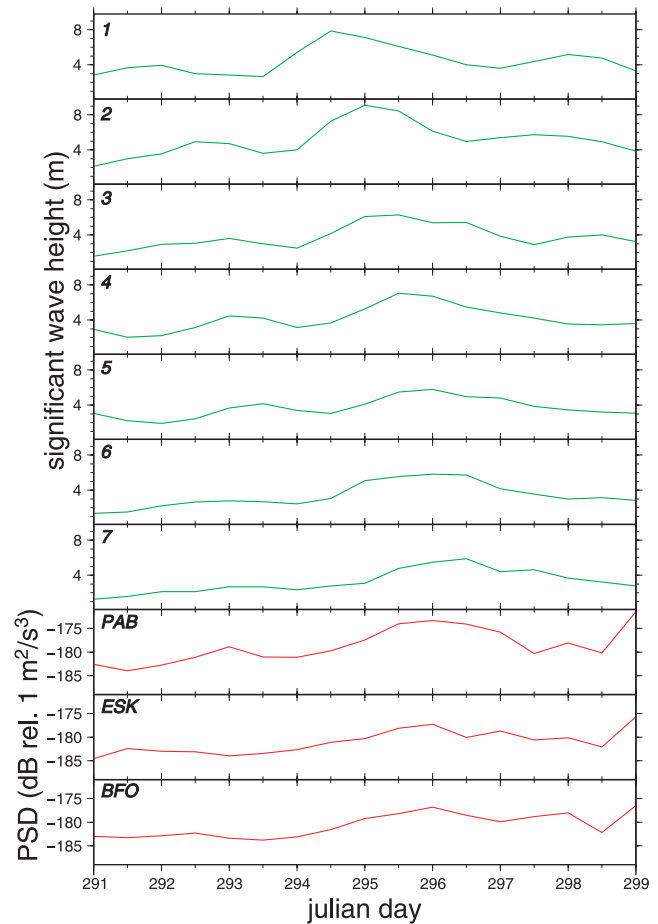


Figure 11. Time-series of significant wave heights (green) and seismic power spectral density (red) at locations shown in Fig. 10.

5. Note that wave height increases earlier at point 3, showing that the seismic excitation occurs near the coastline. At stations BFO and ESK, the seismic noise increases simultaneously and is best correlated with the significant wave height at point 6. In accordance with Fig. 8, Fig. 11 provides strong evidence that the observed long-period Rayleigh waves are not caused by extreme waves in the deep ocean. The interaction of ocean waves with the shallower coastal regions is crucial for the coupling between ocean waves and seismic waves.

In this paper, we study the relations between short period ocean waves and long-period seismic waves. A possible link between these different kinds of waves could be oceanic infragravity waves. As mentioned above, these waves are assumed to be important for the excitation of the Earth's hum. Since on the other hand it has been shown (e.g. Webb *et al.* 1991) that high short period ocean waves cause infragravity waves, it is likely that infragravity waves were present during the storm in the North Atlantic Ocean and played a role for the seismic excitation we observed. However, since there are no direct measurements of infragravity waves available for this event, we cannot further examine this assumption.

3 FURTHER EVENTS

In the preceding section, we intensely studied the complex relations between microseisms, long-period seismic noise and a single storm over the North Atlantic Ocean. We showed that high ocean waves reaching shallow water areas can cause long-period Rayleigh waves

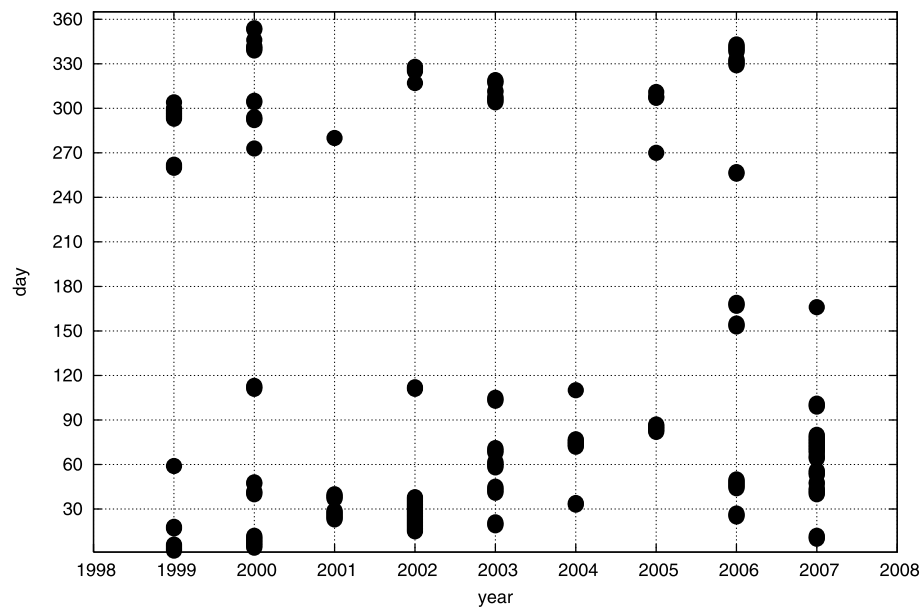


Figure 12. Overview of storms in the North Atlantic Ocean that generated long-period Rayleigh waves between 1999 and 2007.

in the same frequency band where the Earth's hum, the permanent excitation of normal modes, is observed. If such storms were the source of the Earth's hum, they should occur much more regularly to sustain these permanent background oscillations at a constant level. To search for other events similar to the one described above, we compared distributions of beam power as in Fig. 4, determined from the GRSN data, and WAM significant wave height nowcasts as shown in Fig. 8. Between the beginning of 1999 and the mid of 2007, we could identify more than 40 of such events defined as a simultaneous detection of Rayleigh waves arriving from the west and a storm causing high ocean waves in the North Atlantic Ocean. No Rayleigh wave detection without a concurrent ocean storm was made. An overview of these events is shown in Fig. 12.

Most of the events have a duration of only 1–3 d. In some periods, as in 2002 January to February or 2007 February to March, we found a long-standing excitation of seismic waves. From inspection of the WAM nowcasts it is clear that these are sequences of individual storms following close to each other. The frequency of the events obviously depends on season. All but three of them occur between September and April, that is, between autumn and spring. The three events identified in 2006 and 2007 June were less pronounced than the others and are likely to be exceptional. As already mentioned in Section 2, the spectrograms of all events in Fig. 12 show the same characteristics as in Fig. 3: Concurrent microseisms at frequencies near 0.05 and 0.1 Hz, followed by an increase of long-period noise and preceded by a smaller secondary microseismic peak at higher frequency. Most likely, the analogy between these sequences is a consequence of similar storm tracks for these events.

4 CONCLUSIONS

We have shown that beside primary and secondary microseisms, strong storms over the North Atlantic Ocean can cause seismic Rayleigh waves at periods larger than 50 s. These Rayleigh waves originate in coastal areas and lead to an increase of seismic noise which can be observed globally. Thus the influence of ocean waves on seismic noise is not limited to the frequencies of microseisms but is extended down to the mHz range. Since such storms are assumed

to be more common in the Pacific and the Southern oceans than in the North Atlantic Ocean, it is likely that such processes are a major source of seismic noise at frequencies between 2 and 20 mHz, that is, of the Earth's hum.

ACKNOWLEDGMENTS

We thank Toshiro Tanimoto and an anonymous reviewer for their constructive comments and Manfred Joswig for valuable discussions. We are grateful to the Seismological Observatory Gräfenberg (SZGRF), the Berkeley Seismological Laboratory (BSL), the GFZ Potsdam and the Incorporated Research Institutions for Seismology (IRIS) for producing and distributing high quality seismic data, as well as to the Fleet Numerical Meteorology and Oceanography Center (FNMOC) for providing the WAM models. DK was supported by the Deutsche Forschungsgemeinschaft (DFG) under contract no. WI1549/3.

REFERENCES

- Berger, J., Davis, P. & Ekström, G., 2004. Ambient earth noise: a survey of the Global Seismographic Network, *J. geophys. Res.*, **109**, B11307, doi:10.1029/2004JB003408.
- Bromirski, P.D. & Gerstoft, P., 2009. Dominant source regions of the Earth's "hum" are coastal, *Geophys. Res. Lett.*, **36**, L13303, doi:10.1029/2009GL038903.
- Dziewonski, A.M. & Anderson, D.L., 1981. Preliminary reference earth model, *Phys. Earth planet. Inter.*, **25**(4), 297–356.
- Ekström, G., 2001. Time domain analysis of Earth's long-period background seismic radiation, *J. geophys. Res.*, **106**, 26 483–26 493.
- Fukao, Y., Nishida, K., Suda, N., Nawa, K. & Kobayashi, N., 2002. A theory of the Earth's background free oscillations, *J. geophys. Res.*, **107**(B9), 2206, doi:10.1029/2001JB000153.
- Hasselmann, K., 1963. A statistical analysis of the generation of microseisms, *Rev. Geophys.*, **1**(2), 177–210.
- Kobayashi, N. & Nishida, K., 1998. Continuous excitation of planetary free oscillations by atmospheric disturbances, *Nature*, **395**, 357–360.
- Kurrle, D. & Widmer-Schmidrig, R., 2006. Spatiotemporal features of the Earth's background oscillations observed in central Europe, *Geophys. Res. Lett.*, **33**(24), L24304, doi:10.1029/2006GL028429.

- Kurrle, D. & Widmer-Schmidrig, R., 2008. The horizontal hum of the Earth: a global background of spheroidal and toroidal modes, *Geophys. Res. Lett.*, **35**(6), L06304, doi:10.1029/2007GL033125.
- Longuet-Higgins, M.S., 1950. A theory of the origin of microseisms, *Phil. Trans. R. Soc. A*, **243**(857), 1–35.
- Nishida, K. & Fukao, Y., 2007. Source distribution of Earth's background oscillations, *J. geophys. Res.*, **112**, B06306, doi:10.1029/2006JB004720.
- Nishida, K., Kobayashi, N. & Fukao, Y., 2002. Origin of Earth's ground noise from 2 to 20 mHz, *Geophys. Res. Lett.*, **29**(10), 1413, doi:10.1029/2001GL013862.
- Nishida, K., Kawakatsu, H., Fukao, Y. & Obara, K., 2008. Background Love and Rayleigh waves simultaneously generated at the Pacific Ocean floors, *Geophys. Res. Lett.*, **35**(16), L16307.
- Peterson, J., 1993. Observations and Modeling of Seismic Background Noise, *U.S. Geol. Surv., Open-File Rep.*, **93–322**, 1–45.
- Rhie, J. & Romanowicz, B., 2004. Excitation of earth's incessant free oscillations by Atmosphere–Ocean–Seafloor coupling, *Nature*, **431**, 552–556.
- Rhie, J. & Romanowicz, B., 2006. A study of the relation between ocean storms and the Earth's hum, *Geochem. Geophys. Geosyst.*, **7**, Q10004, doi:10.1029/2006GC001274.
- Suda, N., Nawa, K. & Fukao, Y., 1998. Earth's background free oscillations, *Science*, **279**, 2069–2091.
- Tanimoto, T. & Um, J., 1999. Cause of continuous oscillations of the Earth, *J. geophys. Res.*, **104**, 28 723–28 739.
- Tanimoto, T., 2005. The oceanic excitation hypothesis for the continuous oscillations of the Earth, *Geophys. J. Int.*, **160**, 276–288, doi:10.1111/j.1365-246X.2004.02484.x.
- WAMDI group, 1988. The WAM model—a third generation ocean wave prediction model, *J. Phys. Oceanogr.*, **18**, 1775–1810.
- Webb, S.C., 2007. The Earth's 'hum' is driven by ocean waves over the continental shelves, *Nature*, **445**, 754–756, doi:10.1038/nature05536.
- Webb, S.C., 2008. The Earth's hum: the excitation of Earth normal modes by ocean waves, *Geophys. J. Int.*, **174**, 542–566, doi:10.1111/j.1365-246X.2008.03801.x.
- Webb, S.C., Zhang, X. & Crawford, W., 1991. Infragravity waves in the deep ocean, *J. geophys. Res.*, **96**(C2), 2723–2736.
- Wiechert, E., 1904. Verhandlungen der zweiten internationalen seismologischen Konferenz, *Gerlands Beitr. Geophys.*, *Erg.bd. II*: 41–43.
- Zürn, W. & Wielandt, E., 2007. On the minimum of vertical seismic noise near 3 mHz, *Geophys. J. Int.*, **168**(2), 647–658, doi:10.1111/j.1365-246X.2006.03189.x.